AN ATTEMPT TO VALIDATE THE CONCRETE PERFORMANCE TEST WITH THE DEGREE OF AAR-INDUCED DAMAGE OBSERVED IN CONCRETE STRUCTURES

Andreas Leemann [1*], Christine Merz[2]

[1]Empa, Dübendorf, Switzerland

[2]TFB, Wildegg, Switzerland

Abstract

Temperature is increased to accelerate AAR in the concrete performance test (CPT) possibly leading to reaction of aggregates that are non-reactive in concrete structures. In this study, a validation of the CPT according to AFNOR 18-454 was attempted by reproducing the concrete of damaged structures. These concrete mixtures were subjected to the concrete performance test. Measured expansions were compared with the crack width observed in the structures. Moreover, the reacted rock types leading to the expansion were identified in the concrete from the structures and in the lab concrete. The chemical composition of the reaction products was determined in both types of concrete. The agreement of measured expansion, reacted rock types and the composition of the reaction products clearly indicates that the reaction mechanisms in the structure and in the concrete performance test are comparable. As such, the concrete performance test seems to be an appropriate tool to test the potential reactivity of specific concrete mixtures.

Keywords: alkali aggregate reaction, concrete performance test, validation

1 INTRODUCTION

Various concrete performance tests are used today to determine the potential reactivity of specific concrete mixtures [eg. 1,2]. Based on the results of these tests potentially reactive concrete can be distinguished from non-reactive concrete. As such, these tests are an important tool to develop mix designs that prevent alkali-aggregate reaction in new structures. In these tests, AAR is accelerated by increasing relative humidity and temperature. The increase in relative humidity ensures the availability of sufficient moisture for AAR to proceed [3]. The increase in temperature has two effects. On one side, the solubility of SiO_2 increases with temperature [4,5]. On the other side, an elevated temperature during cement hydration leads to an increased pH in the pore solution [6]. Because SiO_2-solubility increases with pH [4,7,8], SiO_2 dissolution is further increased. As a result, the temperature increase may cause a reaction of aggregates in the CPT that are non-reactive in the structure. Therefore, a validation of the expansion obtained in the concrete performance test with the degree of damage observed in concrete structures is mandatory.

Based on the results of concrete properties and concrete composition obtained from damaged structures, concrete mixtures with a similar composition as the on-site concrete are produced in this study. They are tested with the concrete performance test at 60 °C (CPT, [2]). Their expansion is expected to be above the limit value, leading to a classification as potentially reactive. Furthermore, the expansion resulting in the CPT is compared with the crack width observed in the structures. In a complementing approach, the

* Correspondence to: andreas.leemann@empa.ch

reaction frequency of specific rock types present in the aggregates from mixed fluvio-glacial gravel deposits is determined in the concrete of the structures and in the laboratory concrete by optical microscopy. The composition of the reaction products determined with EDX analysis in both laboratory and on-site concrete is compared.

2 MATERIALS AND METHODS

2.1 General

Crack width measurements on on-site concrete, results of the CPT, and microstructural analysis are presented in this paper. This study is part of a larger project where additionally the reactivity of the same aggregates as used in the CPT was determined with the microbar test [9], including a microstructural analysis of the tested specimens, and measurements of the residual expansion potential of the on-site concrete produced with the same aggregates.

Structures from different parts of Switzerland covering different geological settings were selected (Figure 1). All structures exhibit damages due to AAR, except structure GU which was selected as a reference for an undamaged on-site concrete. The age of the investigated structures ranges from 25 to 40 years. In order to reproduce the concrete of the damaged structures, cores were taken using same procedure for all structures; a strongly damaged and a weakly damaged area were selected. Cores with a diameter of 50 and 100 mm were taken from both areas. Based on the mechanical properties of the concrete, its porosity and thin section analysis (data not presented in this paper), cement content and water-to-cement ratio (w/c) were estimated (Table 1). The grain size distribution of the aggregates was assessed visually on the concrete cores by comparing the cores with cores of concrete with a known grain size distribution. Since documents from the construction phase were only partially available, the origin of the cement is not known in one case (structure MS). Moreover, some of the cement plants that delivered the cement for the structures are not in operation any more. In such a case cement with a similar composition was chosen. All structures were built using ordinary Portland cement (CEM I according to EN 197-1). The Na_2O-equivalent in the Swiss cements CEM I has no significant variation and ranges from 0.6 to 1.0 mass-%. As all quarries delivering the aggregates for the structures are still in operation, there was no problem to use aggregates from the same source as used in the specific on-site concrete.

2.2 Materials and mixture proportions

One series of concrete was produced with a cement (CEM I) content of 300 kg/m^3, the other with a cement content of 400 kg/m^3 to cover the range of cement content estimated to be present in the on-site concrete (Tables 1 and 2). As the maximum grain size in the CPT according to AFNOR P 18-454 is limited to 22 mm, the grain size distribution of concrete GU, MS, VI and ME reflects the grain size distribution of the corresponding on-site concrete only up to 22 mm. The CPT requires the addition of NaOH to the mixing water to cover the variability of the alkali content of the cements. 25% of the alkali content of the cement was added as NaOH as prescribed by AFNOR P 18-454. The specimens were produced according to AFNOR P 18-454.

2.3 Methods for assessment and analysis

Crack measurements on the structures

The areas in the structures showing the highest and lowest degree of damage were selected. Widths of the cracks present on the surface of the concrete structures were determined according to [10] using a ruler with pre-drawn bars (width: 0.05-3.5 mm). A square with a side length of 1 m is drawn on the concrete surface. Crack width is measured along two sides of the square and the two diagonals. A crack-index was

calculated as width of crack per measured length. The crack width measured in strongly damaged parts of the structures are regarded as meaningful values to characterise concrete expansion [11,12] and were therefore used in the comparison with CPT expansions.

Concrete performance test

The potential alkali-aggregate reactivity of the concrete was determined according to AFNOR P 18–454 [1]. Three prisms (70 × 70 × 282 mm^3) were produced, stored at 20 °C and demoulded after 24 h. Afterwards, they were stored at 60 °C and 100 % relative humidity for 20 weeks. Every four weeks, their mass and length was measured at 20 °C (cooling period of 24 h). When the expansion after 20 weeks exceeds 0.02% (mix designs with CEM I), the concrete is classified as unsuitable for the use in structures according to AFNOR P 18-456 [13]. This test method is very similar to RILEM AAR 4 which has been assessed in an extensive study conducted by a number of international laboratories as a very consistent method that clearly identifies alkali aggregate reactivity [14].

Optical microscopy

Sections of the different cores from a depth (distance from the concrete surface) > 15 cm were selected and cut to dimensions of 15 × 50 × 90 mm^3. They were dried in an oven at 50 °C for three days, impregnated with epoxy resin containing a fluorescent dye and polished before preparing thin sections with a thickness of approximately 20 μm. Using a Zeiss Axiophot they were studied at a magnification of 25 × and 50 × both in transmitted light with crossed polars and in reflected light with a filter enabling the activation of the fluorescent dye. The latter facilitated the identification of cracks. As for the petrography, between 200 and 450 particles with a diameter > 2 mm were identified both in the on-site concrete (area with strong damage) and in the lab concrete (mixtures with 400 kg/m^3 of cement after the CPT). After determining the petrography of the particles > 2 mm, the petrography was redone taking into account only reacted particles. Classified as "reacted" were particles containing reaction products in cracks and/or exhibiting cracks running from the particles into the paste. The number-% of reacted particles were normalized to 100 % and the difference to the total aggregates present was calculated (Table 3). Consequently, aggregates reacting frequently result in a positive value and aggregates that do not react or react only rarely in a negative value. This analysis was made for the structures MF, ME and VI. This analysis is suited to identify problematic rock types in aggregates consisting of various rock types. Moreover, it permits a comparison of reacting rock types between the on-site and the lab concrete. The other structures were not suited for such an analysis as the aggregates consisted only of gneiss (structure MS) or because an insufficient number of reacted aggregates was present in the concrete for a representative analysis (structures GU, MA and UR).

EDX analysis

Sections of the different cores from a depth (distance from the concrete surface) > 15 cm were selected and cut to dimension of approximately 15 × 40 × 40 mm^3. They were dried in an oven at 50 °C for three days, impregnated with epoxy resin, polished and carbon coated. The analysis of the AAR-reaction products was conducted with an environmental scanning electron microscope (ESEM-FEG XL30). The carbon-coated samples were studied in the high-vacuum mode (2.0-6.0 × 10^{-6} Torr) with an accelerating voltage of 10 kV and a beam current of 180-200 mA. The chemical composition was determined with energy dispersive X-ray spectroscopy (EDX). An EDAX 194 UTW detector, a Philips digital controller, and Genesis Spectrum Software (Version 4.6.1) with ZAF corrections were used. Only reaction products in the core areas of aggregates were analysed, as the reaction products often show considerable calcium uptake close to their rim [15]. To limit the extent of the interaction volume to the reaction products only reaction products in

cracks wider than 5 µm were selected for analysis. In fact, in cement hydrates the interaction volume with the chosen acceleration voltage is typically in the range of 1-3 µm [16]. The chemical composition of the reaction products was studied in 6-8 different aggregates summing up to 100-200 point analysis per concrete. Two structures with a broad range of different rock types in the aggregates (MF and VI) and one structure with gneiss aggregate (MB) were chosen for analysis.

3 RESULTS

Crack measurements

The crack widths in strongly damaged areas of the structures differ significantly between the different structures. The values are expressed as expansion per meter and year for comparison (Table 4). The reference structure for non-reactive concrete has the lowest expansion rate, while structure MS displays the highest values.

Concrete performance test

At a cement content of 300 kg/m^3, four of seven concrete mixtures already exceed the limit value (Figure 2a). Aggregate MS leads to a particular high expansion. At a cement content of 400 kg/m^3 all concrete mixtures except the one with aggregate GU used as non-reactive reference reach expansions above the limit value of 0.02 % (Figure 2b). The increase in cement content increases the expansion of all concrete mixtures. However, the observed increase is especially pronounced in the concrete produced with aggregate VI.

Optical microscopy

In structure MF, quartz-bearing limestone and rhyolite show the most frequent reaction while sandstone reacts only rarely (Figures 3a-c). The same behaviour is observed in the lab concrete, with gneiss being the exception. Gneiss shows a low tendency to react in the structures but a high one in the lab concrete.

Siliceous limestone and quartz-bearing limestone are the rock types reacting most frequently in structure ME. At the other end of the scale is limestone; as it does not contain SiO_2 other than as impurities, it cannot expand significantly. The lab concrete reflects the situation in the on-site concrete: generally, the same rock types show a high and a low frequency to react. However, the values of the lab concrete are considerably higher compared to the on-site concrete.

Again siliceous limestone and quartz-bearing limestone are the frequently reacting rock types in structure VI. Gneiss and limestone react only rarely or do not react. The values for the lab concrete are similar.

The number of reacted aggregates is generally higher in the on-site compared to the lab concrete (Table 5).

EDX analysis

The differences in the chemical composition of the reaction products are relatively small (Table 6, Figures 4a-f). Their silicon content ranges from 60.9 to 75.2 mol-%, calcium content from 12.5 to 22.2 mol-% and alkali content from 11.4 to 19.5 mol-%. The highest Ca/Si-ratio is present in lab concrete MF (0.31) and the lowest in lab concrete MB (0.17). Na/K-ratio displays a range of 0.29 to 0.47 in the on-site concrete and 0.17 to 0.31 in the lab concrete.

Assessed qualitatively, the reaction products in cracks within the aggregates are significantly more common in the on-site concrete than in the lab concrete. On the other hand, gaps at the interface between

paste and aggregate and in voids in the paste close to the interface are more often filled with reaction products in the lab concrete than in the on-site concrete.

4 DISCUSSION

Reproducing the on-site concrete of damaged structures and subjecting these concrete mixtures to the CPT mostly leads to expansions above the limit value. This is an indication that the CPT is able to assess if a specific concrete mixture is potentially reactive or not. Moreover, expansions in the CPT and expansion rates based on crack width measurements on the structures show the same trend (Figure 5). Obviously, the CPT can give an approximation about the degree of expansion that can occur in structures. Of course such a comparison can only show a reasonable fit when the AAR in the structure has already reached a well advanced stage. Despite trying to reproduce the on-site concrete as good as possible, some differences in composition could not be prevented. However, it appears that the variations and changes in the last decades of both petrography of aggregates from the same quarry and changes in cement properties do not have a significant influence on the results. The increase in expansion caused by increasing the cement content from 300 to 400 kg/m^3 depends on the specific aggregate used, indicating that the amount of quartz dissolution and the development of strain in the concrete are not correlated linearly. Although, the concrete of structure GU used as reference for undamaged concrete shows little expansion, more concrete mixtures of this kind are needed to prove that the CPT cannot give false positives. However, the experiences in Switzerland with the Midland gravels indicate that critical cement contents are only reached at approximately 450 kg/m^3 and above.

The temperature increase in the lab test (60° C) to accelerate AAR does not lead to a reaction of rock types that are not reacting in the structure. This is clearly indicated by the agreement of the pattern of rock types with frequent or rare reaction between on-site and lab concrete. On the contrary, the microbar test running at 150° C poorly correlates to the CPT and to the damage observed in field concrete [17]. This is a further indication that the AAR in the structure is well reflected in the CPT. However, differences have to be pointed out as well. Firstly, the number of aggregates reacting in the CPT is in some cases significantly lower than in the structure. One reason could be the test duration of 20 weeks, which is not sufficient for a number of aggregates to generate enough pressure to form cracks. Chemical analyses of the cores did not indicate a significant leaching of alkalis which might have explained the different behaviours in any case. Secondly, the qualitatively assessed differences in the local occurrence of reaction products can be explained with the differences in the temperature. The gelation process accelerates at high temperatures, but the viscosity of silica gel is decreasing with increasing temperature [18]. As a result, the extrusion of reaction products from the aggregates into the paste (with causing little or no cracking), is more frequent in the lab concrete.

In regard to the ratio between silicon, calcium and the sum of potassium and sodium, the reaction products are very similar, despite the differences in exposure and age. This indicates that the reaction mechanisms are comparable as well. The Ca/Si-ratio of the reaction products defines their ability to take up water and swell [19-21] indicating similar properties in this aspect of the analysed reaction products. The variations in the Na/K-ratio is in a similar range and are likely caused by the alkalis available in the pore solution [22] and possible some alkali release by reacting minerals []. The number of analysed aggregates and of point analyses might not have been sufficient to be representative for the Na/K-ratio. In general, the composition of the reaction products correlates with the one reported in literature [eg. 22-24].

5 CONCLUSIONS

Reproducing the concrete of damages structures, testing it with the CPT and analysing lead to the following findings:

- The majority of the lab concrete mixtures exceeds the limit value for expansion at a cement content of 300 kg/m^3, while all concrete mixtures except the non-reactive reference exceed it at a cement content of 400 kg/m^3.
- Expansion rates determined with crack measurements on the structures and expansion in the CPT show a good correlation.
- The same rock types react frequently respectively rarely in on-site and lab concrete.
- The chemical composition of the reaction products is very similar in both structural and lab concrete.

Obviously, non-reactive and potentially reactive concrete mixtures can be distinguished with the CPT. Furthermore, the determined expansion can give an indication about the degree of expansion possible in the structure. As such the CPT is an important tool to develop mix designs for non-reactive concrete and to prevent future damages.

6 ACKNOWLEDGEMENT

The aouthors would like to thank the federal road authorities (ASTRA) for the financial support of the project (AGB 2005/023, AGB 2006/03).

7 REFERENCES

[1] ASTM C 1260-01(2004) Standard test method for potential alkali reactivity of aggregates (mortar-bar method). Annual book of ASTM standards (04.02), 680–684.

[2] AFNOR P18-454 (2004): Réactivité d'une formule de béton vis-à-vis de l'alcaliréaction (essaie de performance). Association Française de Normalisation, Paris.

[3] Olafson, H (1986): The effect of relative humidity and temperature on alkali expansion of mortar bars. In: Concrete alkali aggregate reactions. Noyes publications, Far Ridge, NJ, 461-465.

[4] Dove, PM (1994): The dissolution kinetics of quartz in sodium chloride solutions at 25° to 300 °C. American Journal of Science (294): 665–712.

[5] Icenhower, JP, and Dove, PM (2000): The dissolution kinetics of amorphous silica into sodium chloride solutions: effects of temperature and ionic strength. Geochimica and Cosmochimica Acta (64) 4193–4203.

[6] Lothenbach, B, Winnefeld, F, Alder, C, Wieland, E, and Lunk, P (2007): Effect of temperature on the pore solution, microstructure and hydration products of Portland cement pastes. Cement and Concrete Research (37): 483-491.

[7] Alexander, GB, Heston, WM, and Iler, RK (1954): The Solubility of Amorphous Silica in Water. The Journal of Physical Chemistry (58): 453–455.

[8] Mazer, JJ, and Walthera, JV (1994): Dissolution kinetics of silica glass as a function of pH between 40 and 85°C. Journal of Non-Crystalline Solids (170): 32-45.

[9] AFNOR P18-588 (1991): Granulats - stabilité dimensionnelle en milieu alcalin (essai accéléré sur mortier MICROBAR). Association Française de Normalisation, Paris.

[10] LCPC (1997): Détermination de l'indice de fissuration d'un parement de béton. Méthode d'essai LPC 47.

[11] Godart, B, Mahut, B, Fasseu, P, and Michel, M (2004): The guide for aiding to the management of structures damaged by concrete expansion in France. In: Tang, M, and Deng, M (editors): Proceedings of the 12th ICAAR, Bejing, China: 1219-1228.

[12] Vézina, D, and Bouchard, D (2006): Concrete highway structures showing signs of ASR distress: monitoring program at the Ministère des Transports du Québec. In: Fournier, B (editor): Marc-André Bérubé Symposium on Alkali-Aggregate Reactivity in Concrete. Montréal, Canada: 413-422.
[13] AFNOR FD P18-456 (2004): Réactivité d'une formule de béton vis-à-vis de l'alcaliréaction. Association Française de Normalisation, Paris.
[14] Nixon P, Lane S (2006): Experience from testing of the alkali reactivity of European aggregates according to several concrete prism test methods. Partner report 3.3 (n SBF52 A06021). Trondheim: SINTEF.
[15] Katayama, T (2008): ASR gel in concrete subject to freeze-thaw cycles - comparison between laboratory and field concretes from Newfoundland, Canada. In: Proceedings of the 13th International Conference on Alkali-Aggregate Reaction in Concrete, Trondheim, Norway: 174-183.
[16] Wong, HS, and Buenfeld, NR (2006): Monte Carlo simulation of electron-solid interactions in cement-based materials. Cement and Concrete Research (36) 1076–82.
[17] Leemann, A, and Merz, C (2012): Comparison between AAR-induced expansion determined with an ultra-accelerated microbar test and a concrete performance test. Submitted to the 14th ICAAR.
[18] Amiri, A, Øye, G, and Sjöblom J (2011): Temperature and pressure effects on stability and gelation properties of silica suspensions. Colloids and Surfaces A: Physicochemical and Engineering Aspects (378): 14-21.
[19] Wieker, W, Hubert, C, Heidemann, D, and Ebert, R (1998): Alkali–aggregate reaction- a problem of the insufficient fundamental knowledge of its chemical base. In: Cohen, M, Mindess, S, and Skalny, J (editors): Proceedings of the Sidney Diamond Symposium on Materials Science and Engineering of Concrete and Cementious based Composites. Materials Science of Concrete, American Ceramic Society, Westerville, OH: 395–408.
[20] Mansfeld, T (2008): Das Quellverhalten von Alkalisilikatgelen unter Beachtung ihrer Zusammensetzung (Expansion behaviour of alkali silicate gels considering their composition), Doctoral Thesis, Bauhaus-Universität Weimar, Germany.
[21] Leemann, A, Le Saout, G, Winnefeld, F, Rentsch, D, and Lothenbach B (2011): Alkali–silica reaction: the influence of calcium on silica dissolution and the formation of reaction products. Journal of the American Ceramic Society (94) 1243–1249.
[22] Leemann, A, and Lothenbach, B (2008): The influence of potassium–sodium ratio in cement on concrete expansion due to alkali-aggregate reaction. Cement and Concrete Research (38): 1162–1168.
[23] Thaulow, N, Jakobson, UH, and Clark, B (1996): Composition of alkali silica gel and ettringite in concrete railroad ties: SEM-EDX and X-ray diffraction analysis. Cement and Concrete Research (26): 309-318.
[24] Knudsen, T, and Taulow, N (1975): Quantitative microanalyses of alkali-silica gel in concrete. Cement and Concrete Research (5): 443-454.

TABLE 1: Location, type and abbreviated name of the investigated structures with a simplified petrography of the aggregates (n.a. = not analysed, aggregate $Ø_{max}$ = maximum grain size used in structure.

region and county	location, type of structure, year of construction	cement content [kg/m³]	w/c	aggregate $Ø_{max}$ [mm]	label of aggregate and structure	present rock types (in order of decreasing amount)
Midland, Solothurn	Wangen, viaduct, 1977	325-350	0.45-0.50	32	GU	sandstone, quartzite, gneiss, siliceous limestone, limestone
Jura, Neuchâtel	Thielle, supporting wall, 1970/77	350-400	0.43-0.45	22	MA	limestone, limestone with detritic quartz, gneiss, sandstone, siliceous limestone, quartzite
Alps, Wallis	Mattsand, dam, 1963	400	0.45-0.50	60	MS	gneiss
Prealps, Vaud	Bornisses, supporting wall, 1967-68	400	0.45-0.50	32	VI	limestone with detritic quartz, siliceous limestone, gneiss, quartz, limestone, schist
Prealps, Uri	Rorbach, bridge, 1982-83	350-400	0.45-0.50	20	UR	gneiss, siliceous limestone, sandstone, schist, limestone with detritic quartz, quartzite
Prealps, St. Gallen	Mels, viaduct, 1969	300-350	0.45	20	MF	limestone with detritic quartz, sandstone, gneiss, quartzite, schist, granophyr
Prealps, Vaud	Mur 10, supporting wall, 1980	400	0.43-0.45	32	ME	limestone with detritic quartz, siliceous limestone, limestone, sandstone, gneiss, quartzite, silex

TABLE 2: Concrete mixtures.

concrete	cement content [kg/m³]	Na_2O-equ of CEM I without addition of NaOH [mass-%]	w/c
GU	300 / 400	0.79	0.45
MF	300 / 400	0.78	0.45
UR	300 / 400	0.80	0.50
MA	300 / 400	0.90	0.45
MS	300 / 400	0.77	0.50
ME	300 / 400	0.83	0.45
VI	300 / 400	0.83	0.45

TABLE 3: Petrography of aggregate ME (on-site concrete); all aggregates present, the reacted aggregates and their relative difference.

column	A	B	C	D
rock types	total aggregates [number-%]	reacted aggregates [number-%]	reacted aggregates (column B) normalized to 100%) [number-%]	difference between reacted aggregates (column C) and total aggregates (column A [number-%]
gneiss	7.2	2.5	9.4	2.2
quartzite	4.0	0.7	2.7	-1.3
sandstone	5.8	1.1	4	-1.8
siliceous limestone	28.9	8.7	32	3.1
quartz-bearing limestone	46.7	14.1	52	5.3
limestone	7.2	0	0	-7.2
sum	100.0	27.2	100.0	-

TABLE 4: Expansion rate of strongly damaged areas of the structures based on crack width measurements.							
structure	GU	MF	UR	MA	MS	ME	VI
expansion rate [mm/m·y]	0.010	0.035	0.040	0.060	0.100	0.020	0.060

TABLE 5: Amount of reacted aggregates in the on-site and the lab concrete.		
structure	reacted aggregates [number-%]	
	on-site	CPT
MF	30	11
UR	36	<3
ME	27	15
VI	34	35

TABLE 6: Chemical composition of the reaction products analyzed within aggregates of on-site and lab concrete (after the CPT).							
structure	Concrete	Si [mol-%]	Ca [mol-%]	Na [mol-%]	K [mol-%]	Ca/Si	Na/K
MF	on-site concrete	63.3	17.2	6.1	13.4	0.27	0.47
	lab concrete	62.3	19.4	6.6	10.3	0.31	0.39
UR	on-site concrete	68.7	15.0	3.7	12.6	0.21	0.29
	lab concrete	68.1	17.0	1.8	13.1	0.25	0.13
MB	on-site concrete	72.9	15.3	2.7	9.1	0.21	0.30
	lab concrete	75.2	12.5	2.6	9.7	0.17	0.27

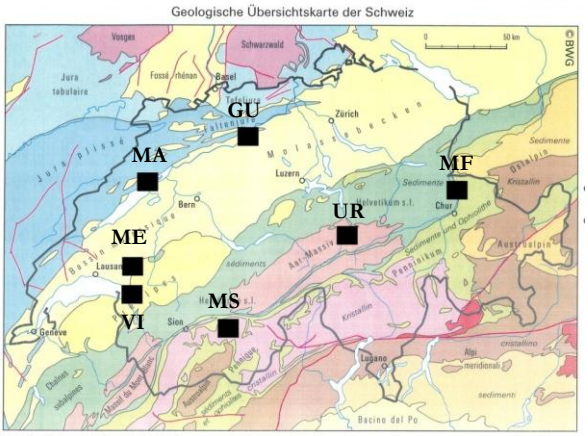

Figure 1: Location of the investigated structures in Switzerland.

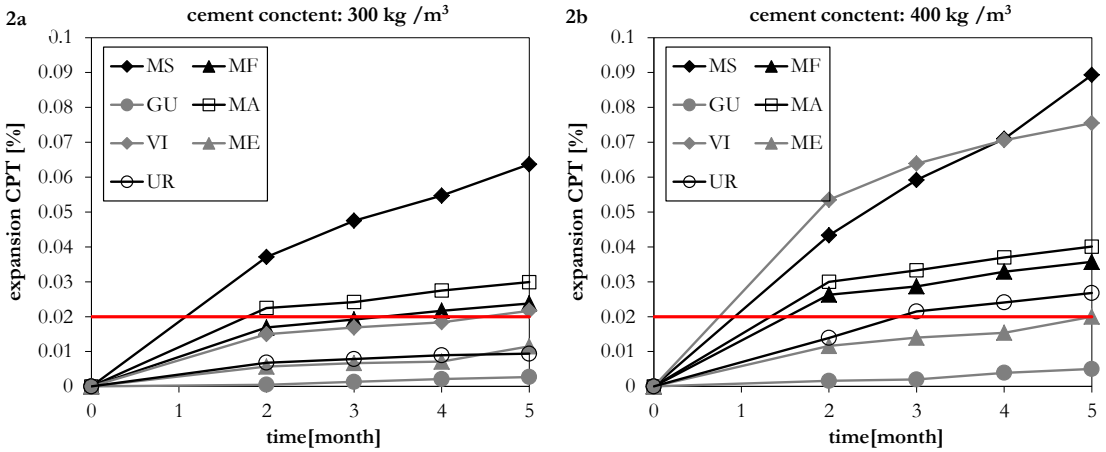

FIGURES 2a and 2b: Expansion of the lab concrete using a cement content of 300 and 400 kg/m³.

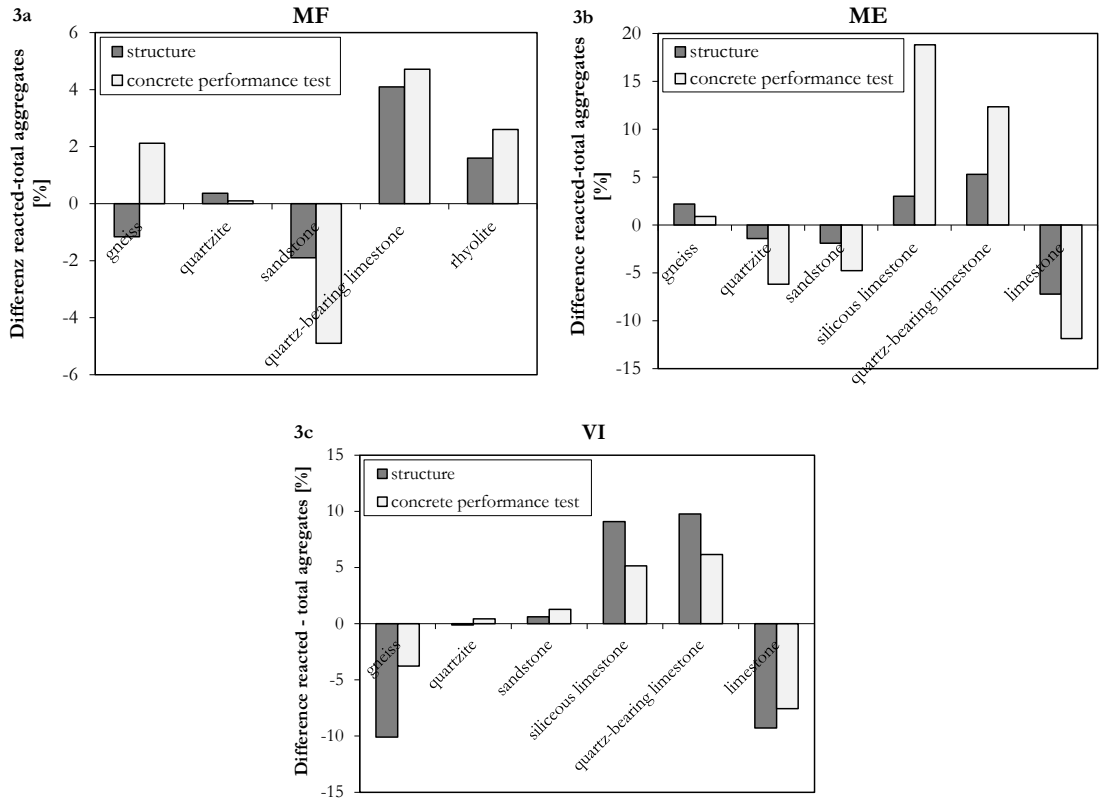

FIGURES 3a-3c: Relative difference between rock types showing above (positive values) or below (negative values) average frequency of reaction in on-site concrete and in lab concrete (after the CPT / structures MF, ME and VI).

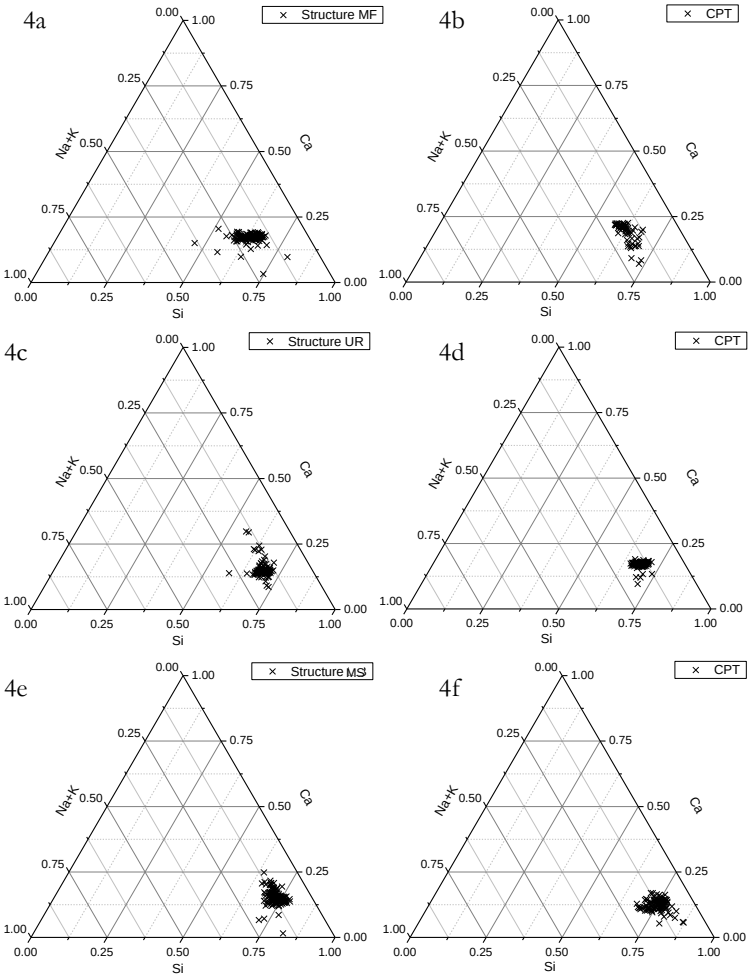

FIGURES 4a-4f: Composition of the reaction products the in on-site concrete and the in lab concrete (CPT) after the test (structures MF, UR and MS).

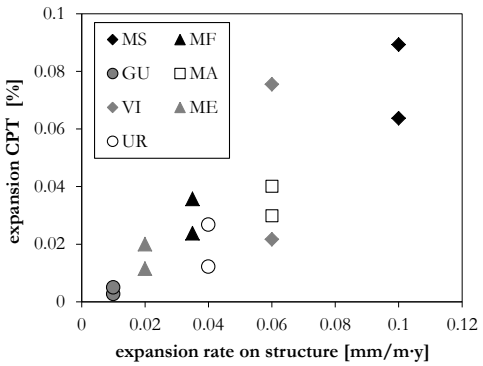

FIGURE 5: Expansion in the CPT as a function of the rate of expansion in the structures assessed by the determination of the crack-index in combination with the age of the structure.